Article

Similarity and Change Detection of Relief in a Proglacial River Valley (Scott River, SW Svalbard)

Leszek Gawrysiak and Waldemar Kociuba *

Institute of Earth and Environmental Sciences, Maria Curie-Skłodowska University in Lublin,
20-031 Lublin, Poland; leszek.gawrysiak@mail.umcs.pl
* Correspondence: waldemar.kociuba@mail.umcs.pl; Tel.: +48-81-537-6853

Abstract: This study focuses on contemporary geomorphic changes in the proglacial valley floor of the Scott River catchment (northwest of Wedel Jarlsberg Land, southwestern Spitsbergen). The similarity and variability of landforms along the entire 3.3 km length of the unglaciated valley floor was assessed using precision terrestrial laser scanning (TLS) measurements made in July/August 2010–2013. Digital terrain models (DTMs) were generated from the high-resolution TLS survey data, followed by a geomorphon map, which was then used for a similarity and changes of morphology analysis performed with GeoPAT2 software. The study revealed a large spatial variation of contemporary processes shaping the valley floor and changes in its morphology. Their spatial distribution relates to the geologically determined split of the valley floor into three morphological zones separated by gorges. The upper gorge cuts the terminal moraine rampart, which limits the uppermost section of the valley floor, which is up to 700 m wide and is occupied by the outwash plain. The study showed that this is the area characterised by the greatest dynamics of contemporary geomorphic processes and relief changes. The similarity index value here is characterised by a large spatial variation that in some places reaches values close to 0. In the middle section stretching between the upper gorge (cutting the terminal moraine) and the lower gorge (cutting the elevated marine terraces), a much smaller variability of processes and landforms is observed, and the found changes of the valley floor relief mainly include the area of braided channel activity. Similarity index values in this zone do not fall below 0.65. The lowest section, the mouth of the alluvial fan, on the other hand, is characterised by considerable spatial differentiation. The southern part of the fan is stable, while the northern part is intensively re-shaped and has a similarity index that locally falls below 0.5. The most dynamic changes are found within the active channel system along the entire length of the unglaciated section of the Scott River. The peripheral areas, located in the outer zones of the valley floor, show grea stability.

Keywords: TLS scanning; high-resolution DTM; geomorphons; GeoPAT2; relief segmentation; clustering; relief similarity and changes

1. Introduction

Global climate change, occurring as a result of increasing average air temperatures [1,2], is manifested in the high-Arctic environment by an increasing rate of cryosphere degradation [3,4]. Small valley glaciers, particularly those with their glacier terminus on land, respond to these changes with dynamic retreat and intense melting of their surfaces [5]. The consequence is an intensification of geomorphic processes that reshape the valleys of the proglacial rivers that drain them [6]. The most evident effect of the melting of the glaciers is a rapid increase of the direct glaciers' foreland, which becomes exposed from under the retreating glacier snout [7]. This area undergoes intensive reshaping under the conditions of the high outflow energy of sub- and supra-glacial waters, supplying large amounts of sediment [8–11]. In the zone of the active braided system, frequent channel shifting and avulsion occur [12], while temporary fans and bars are deposited

in between [13]. The lifetime of these ephemeral landforms is usually very short [7,14], and traditional measurement methods do not allow a full quantitative estimation of these changes [15]. The use of remote-sensing methods, such as satellite imaging, aerial and terrestrial photogrammetry [16], global navigation satellite systems (GNSS) [17], and light detection and ranging (LiDAR) [18–21], is helpful in this regard. Due to the widespread use in studies of environmental change and the complementarity of the latter two methods, the accuracy of measurement has changed from a few metres to a few centimetres [22]. Through a combination of the advantages of GNSS measurements, with which it is possible to create a positioning network of ground control points (GCPs), and the high precision of airborne laser scanning (ALS) or terrestrial laser scanning (TLS) surveys, we can obtain georeferenced terrain models in the form of a point cloud with a density ranging from a few (ALS) to hundreds (TLS) of points per square meter. These models allow the interpretation of relief at different spatial scales [23]. The increasing availability of survey data has led to the development of methods for the quantitative detection of geomorphic changes [24]. One of these is the geomorphons method. This was developed in 2011, when Stepinski and Jasiewicz [25] proposed a new method for relief analysis. The typological units obtained by geomorphons are a computer interpretation of landforms and correspond to all morphological types that can occur in the natural environment [25,26]. These units are determined by classifying the digital terrain model (DTM) and assigning information to each raster cell about its position (elevation) in relation to 8 cells in its (closer or further) surroundings. This process is semi-automatic and requires the operator to specify the search distance parameter. Its proper refinement allows the DTM to be reclassified in relation to the guiding features of the relief of the area and the assumed degree of generalisation [26], which in turn led to the identification of 498 theoretically possible unit types. Due to the rarity of some of these types and the legibility of the resulting geomorphometric map, the authors proposed the classification of all existing types into the 10 most common ones: flat, peak, ridge, shoulder, spur, slope, hollow, footslope, valley and depression. Geomorphons have so far been used for, among other things, the geomorphometric map of Poland [26], and the machine mapping of physiographic units [27,28]. Geomorphons have also been used to analyse the specificity of relief in different morphogenetic zones of Poland and their relation to the geomorphological map [29]. These studies were conducted for large areas (planetary, continental, sub-continental, regional scales), where the size of the basal cell ranged from 90 to 5 m. Gawrysiak and Kociuba [30] have proposed the use of geomorphons for high-resolution models based on TLS-derived DTMs at the local scale. Changing the base cell size from 'km' and 'm' to 'dm' allowed selected sections of the proglacial river valley floor to be analysed using this method [30].

In the current study, a first attempt was made to apply the geomorphons method with the similarity method to analyse the spatial–temporal changes of the entire non-glaciated valley floor of a small proglacial river in the high Arctic. The objectives of the present study were:

(i)   to obtain quantitative information on the rate, magnitude and directions of contemporary relief reshaping of a small proglacial valley under conditions of rapid valley glacier retreat;

(ii)   to develop a typology and to map the valley floor forms using geomorphons;

(iii)   to undertake a similarity analysis of the valley floor surface and a separation of the relatively homogeneous segments for each measurement season;

(iv)   to undertake a similarity analysis of valley floor landforms and an estimation of their variability over a three-year period.

2. Materials and Methods

2.1. Study Area

The study covered a 3.3 km-long unglaciated bed (0.42 km^2) of the proglacial Scott River, which outflows into Recherchefjorden (part of Bellsund Fjord, in the NW part of Wedel Jarlsberg Land (SW Svalbard)) (Figure 1). The river originates from the Scottbreen

valley glacier covering about 40% of the Scott River catchment area of 10 km². The glacier front retreats at a rate of about 20 m each year [7,13]. Scottbreen is the main source (90%) for the proglacial Scott River [31], and the outflow of sub- and supraglacial waters is located in the south-eastern part of the glacier terminus at an elevation of approximately 90 m a.s.l. (Figure 1). The catchment area is geologically and geomorphologically diverse. In the upper section, covered by the Scottbreen glacier, there are partly metamorphosed upper and lower diamictites of the Kapp Lyell Formation, bordered by green and black shales and phyllites, weathered sandstones and conglomerates of the Bergskardet Formation. Those of the clasts within the 'Calypsostrand' tectonic trench are adjacent to Palaeogene sediments covered by Quaternary marine gravels, exposed in the middle and lower sections of the catchment [32]. Quaternary glacial, fluvioglacial and fluvial sediments underlie the unglaciated Scott River valley floor. Geological conditions determine the split of the valley floor into three morphological zones, separated by gorge-like narrowings. The upper gorge cuts the terminal moraine rampart, that bounds the 600–700 m wide uppermost section of the valley floor occupied by the outwash plain, modelled by a braided river and varied by hills of recessional moraine, glacial lakes and a flow-through lake that develops each year during the melt season. In the middle section below the upper gorge, the valley floor, with a width of up to 250 m, is cut into the isostatically elevated marine terraces area of 'Calypsostranda', varying in age and height. The floor relief is dominated by braided channels, whose zone of activity reaches a width of up to 60 m. The lower section of the valley floor is separated from the middle section by the lower gorge, dissecting the lowest elevated marine terraces. Below the gorge, the Scott River forms a mouth alluvial fan that is up to 550 m wide, varied by an extensive system of braided channels and distributaries functioning during melt season. Located at the foot of the alluvial fan, the bank rampart forces a change in the direction of outflow from the SW-NE which dominates the entire length of the unglaciated valley floor to the NW-SE, perpendicular to it. In this section of the river course, which is of several hundred meters, the runoff waters from the alluvial fan join into a single channel that cuts through the rampart in the S part of the fan and drains the Scott River into the Recherchefjorden (Figure 1).

2.2. TLS Scanning (Surveying)

Accurate TLS surveys along the entire length of the Scott River valley floor (approximately 3.3 km long and 1.3 km²) were carried out during two survey campaigns, in 2010 [23] and 2013 [13], using a Leica ScanStation C10 terrestrial laser scanner [33]. This is a scanner with a range of up to 300 m that emits green laser (532 nm) pulses at up to 50 000 points per second [pt/s] [33] that can penetrate water and that is thus well suited for water applications [34]. In both cases, measurements were made in late July/early August during the thermal optimum of the melt season [13,23]. The unglaciated valley floor was first scanned in 2010 in a local reference system. Multi-site scanning was performed from 82 interconnected sites using a network of 86 reference points with an accuracy of ~0.01 m (±9 mm). Black and white targets recognised during scanning by the Leica ScanStation C10 laser scanner interface were used as reference markers. For nine of these points (proportionally distributed over the study area), the position was determined with a Leica 500 dGPS satellite receiver to an accuracy of ±0.02 m. This allowed the entire model to be georeferenced during the scan registration process in Cyclone 8.0 software (Leica Geosystems AG, Heerbrugg, Switzerland) [33]. However, this method, despite its high accuracy, is very time consuming. Therefore, in 2013, a fixed network of 120 reference points positioned with two TopCon Hiper II GNSS receivers (working in a base–rover system) was used [13]. The use of real-time kinematic measurement rtkGNSS (using two satellite positioning systems: the global positioning system (GPS) and the globalnaya navigacionaya sputnikovaya sistema (GLONASS)) with the same positioning accuracy of ±0.02 m as that utilized in 2010, allowed the position of all 120 reference points to be determined. This enabled a more efficient field mode to be used. The position of all reference points in the form of a text file containing position and elevation coordinates (x, y, z) was uploaded to

the Leica ScanStation C10 scanner interface. The reference points (with known coordinates) were located interchangeably between the ScanStation and the target (a 6 inch Leica target) embedded on 1 m survey pole. This method of organising the field survey campaign meant that, while already in the field, we were able to geo-reference all points acquired in the form of a point cloud. An additional advantage of this measurement method is that more scans were taken and the measurement area was extended in the upper section of the valley floor [13]. TLS-derived data from both measurement campaigns were further processed in several postprocessing steps.
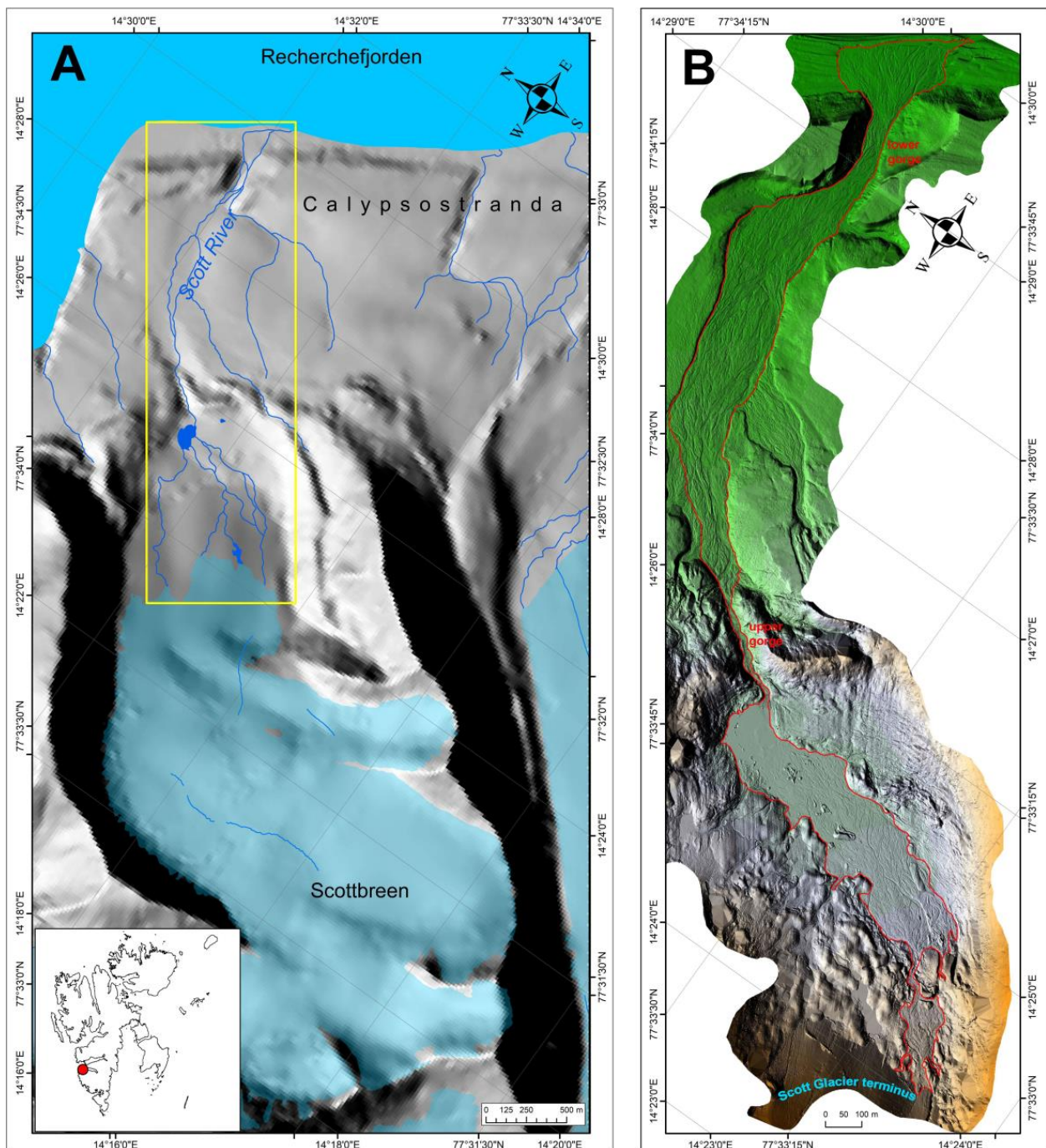

Figure 1. Location of the Scott River catchment in NW Wedel Jarlsberg Land (SW Svalbard); the yellow rectangle limits the extent of the investigated catchment (**A**). Scott River valley study area: the red line limits the extent of the valley floor analysed (**B**).

2.3. Postprocessing and DTM Generation

In both cases, the survey data (point clouds) were registered to a single digital surface model (DSM) in Leica Cyclone 8.0 software (Figure 2). The data were then filtered using the cloth simulation filtering (CSF) algorithm to classify and extract ground points [35]. CSF was used as a plug-in in CloudCompare 2.11 (3D point cloud and mesh processing software (Open Source Project)). The main parameter 'canvas thickness' was set to the lowest possible value of 0.1 m. The classified ground points were then re-imported into Cyclone 8.0 to verify the correctness of the filtering and possibly manually remove noise (non-ground points) missed by the algorithm. The most common were birds, insects and phantoms, i.e., sun reflections and survey infrastructure objects in the 0.1 m ground layer. The correctly classified points were then processed with LP360 7.0 software (GeoCue Group Inc., Huntsville, AL, USA) into a triangulated irregular network (TIN) and then rasterised as Geotiff with cell size 0.1 m. In the next step, the raw rasterised terrain models were loaded into ArcGIS Pro (ESRI, Redlands, CA, USA) and processed with a fill filter to obtain hydrologically correct DTMs. In the next step, the synchronisation of the DTMs was checked and hillshade maps were generated for each model.

2.4. Geomorphon Maps, Relief Clustering and Similarity

The obtained DTMs, from 2010 and 2013, were then used to develop geomorphon maps (Figure 2), using the r.geomorphon function [26] in The Geographic Resources Analysis Support System; Geographic Information System (GRASS GIS 7.6.1) software. In order to produce valid geomorphon maps for analysis, a number of variants of the algorithm were tested with different values of the skip, search and flatness parameters. The resulting maps were visually analysed for correct representation of the relief, especially the ridges and valleys that form the main features of the valley floor morphology. Finally, geomorphon maps, generated with the following parameter values, were selected for further analysis: skip = 2 m, search = 10 m, flatness = 0.5. In the next step, the extent of the Scott Valley floor was mapped by visually interpreting the DTMs and hillshades. The geomorph maps were then cropped to the valley floor boundary. The geomorphon maps from both years in which they were prepared in this way were used in the next step to produce signature files, using the GeoPAT2 software [36]. This programme implements algorithms dedicated to the analysis of large raster sets based on spatial pattern. Signature files (similarity characteristics) and motifs (10 × 10 m resolution) in this programme are created by processing geomorphon maps using the spatial co-occurrence method [37], dedicated to sets with very complex spatial structures, such as geomorphons [36]. The motifs were then grouped into segments i.e., homogeneous areas. A different number of segments was obtained in each of the years analysed, indicating the changes in relief that took place between measurements. Based on the signature files, distance matrices were calculated based on the Jensen–Shanon divergence [38], and were then used to group (hierarchical clustering) segments into classes with a defined degree of similarity [38]. The separation of classes was based on the developed dendrograms (Ward method) assuming the same cut-off height in both diagrams. Similarity maps of the 2010 and 2013 relief were created using the GeoPAT2 software function, which compares signature files based on the Jensen–Shanon divergence [38]. In the final step, zonal statistics were calculated for the segments and similarity maps in order to compile the quantitative characteristics of the analysed datasets (Tables 1–3).
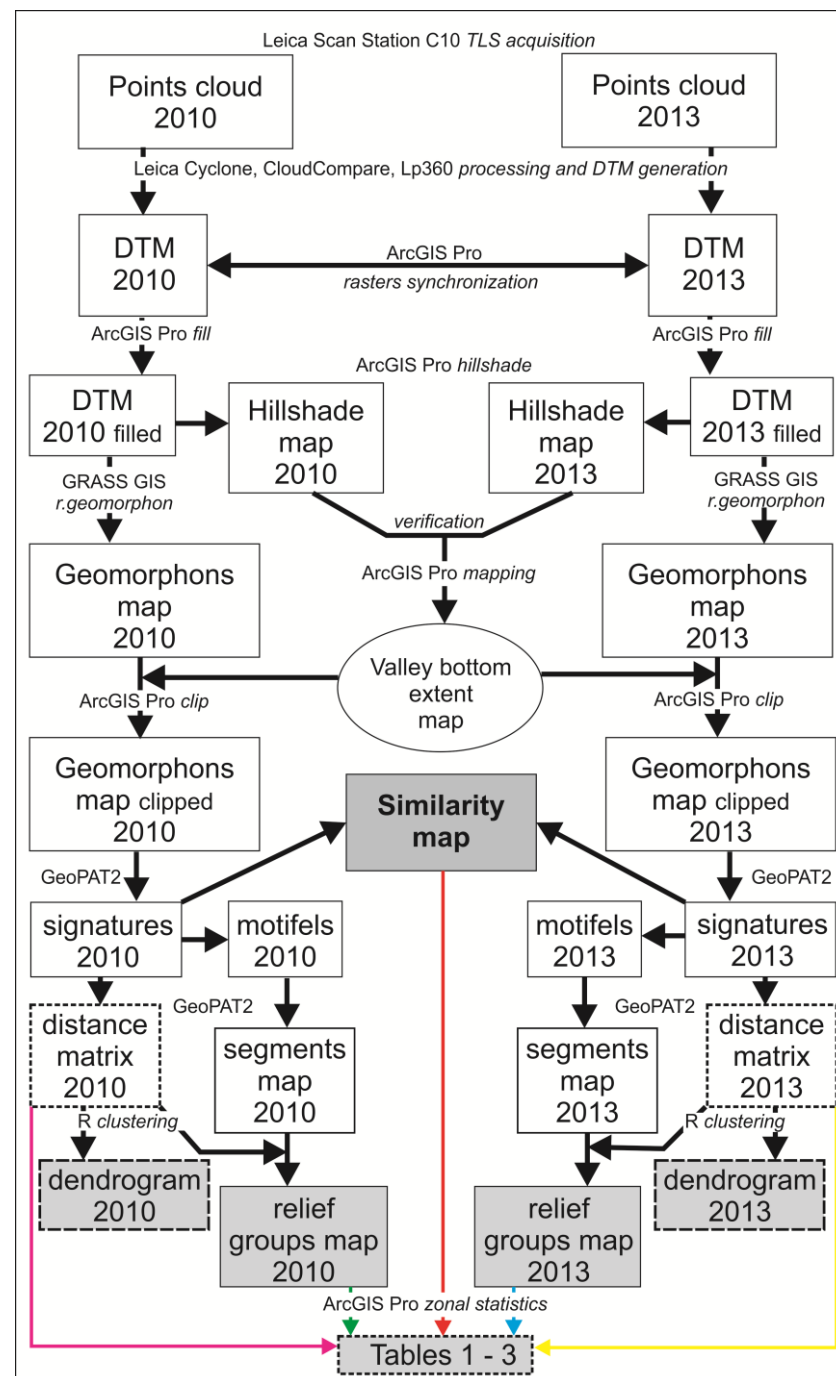
Figure 2. Workflow model of data processing and calculations. Elements marked in grey are included in the text as separate figures and tables.

3. Results

3.1. Relief Classes

3.1.1. The Situation in 2010

The 2010 Scott Valley floor model was divided into 213 segments (Figure 3A,B; Table 1) grouped into 6 classes. Unit-wise, group 1 is the most numerous (85 segments), while in terms of area it is the second most numerous. It occupies the largest area in the upper section of the valley (Figure 3B), and also occurs in the vicinity of the glacier front and in segments below the gorge and at the beginning of the inflow cone. The group is internally differentiated—2 subgroups are marked on the dendrogram (Figure 3A). It is distinguished

from the others by having the highest maximum distance value and a fairly high standard deviation (Table 1). These are indicative of considerable intra-group variation. Group 4 is the second most numerous (62 segments), but has by far the largest area (29.49 ha; 71.04%). Within its internal structure, two subgroups are also clear. It occupies extensive areas in the section below the gorge and on the inflow cone and is "intermingled" with Group 1 above the gorge. Its statistics (Table 1) show the occurrence of quite distinct segments (max = 0.541) with the mean and standard deviation locating it roughly in the middle of all segments. The remaining four groups occupy much smaller areas. Among them, Group 3 stands out, consisting of as many as 40 segments, located in the gorge section and a small throat close to the glacier terminus. Group 5 (6 segments) occupies the area of a periodically functioning flow-through lake located in front of the inlet to the gorge. It has a fairly low mean and standard deviation, indicating its internal similarity. Adjacent to Group 5 (Figure 3B) is Group 2 (16 segments), which occupies the margins of the flow-through lake and has the highest mean and standard deviation supporting its high internal differentiation. The least abundant (4 segments), and with the smallest area (0.15 ha), is Group 6, which occurs only in the vicinity of the Scott Glacier terminus (Figure 1B,3B).
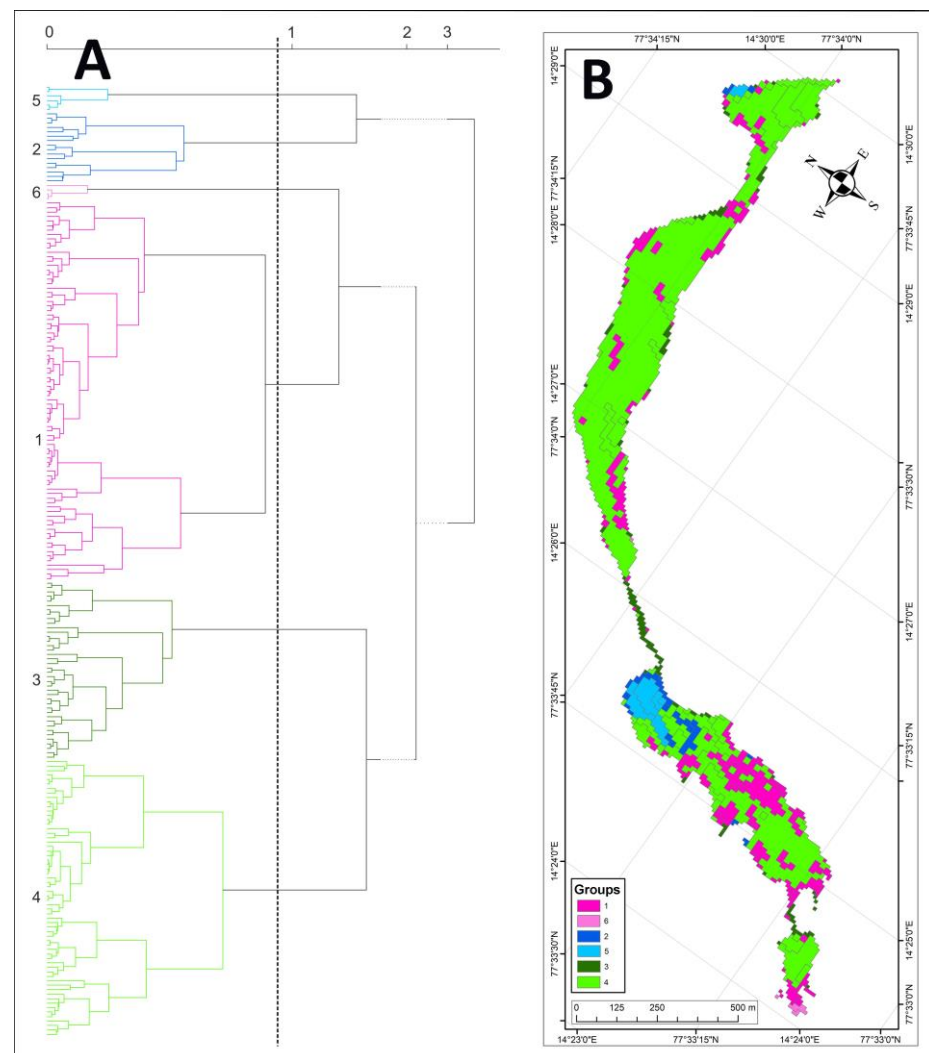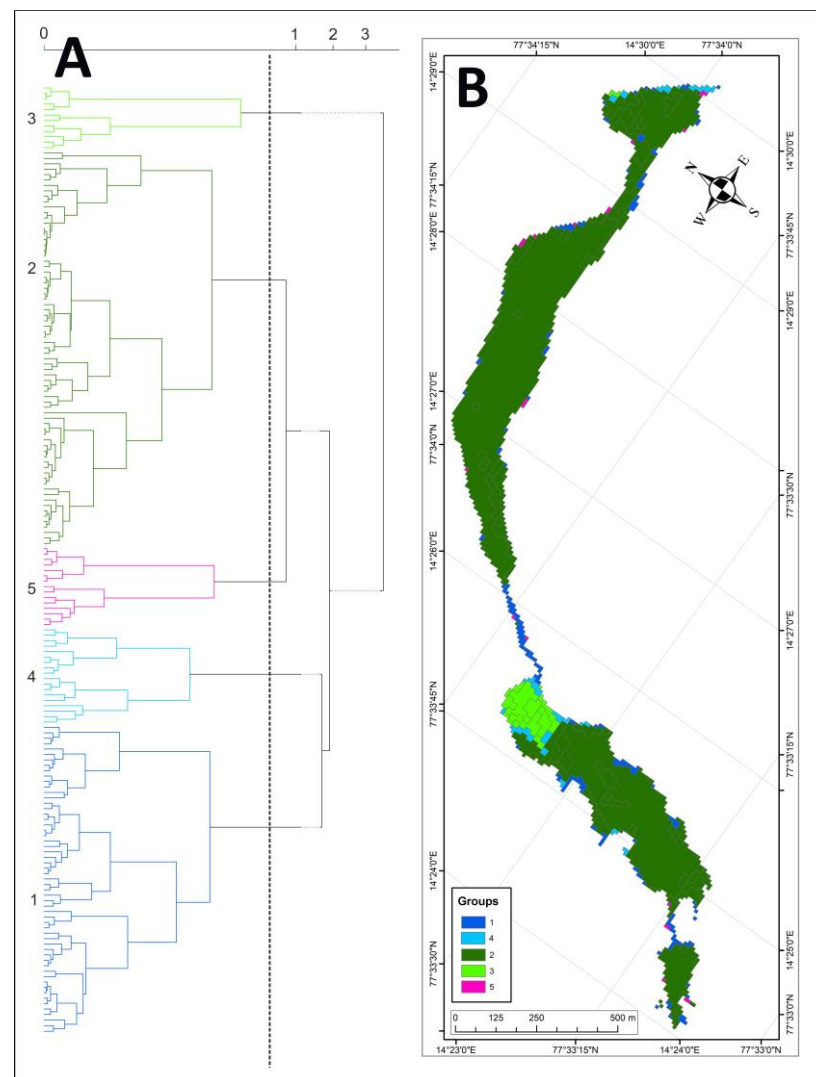

Figure 3. Dendrogram (**A**) and map (**B**) of relief segments (2010) grouped into 6 main groups. The dotted line on dendrogram (**A**) marks the height of cutting.

Table 1. Area and changeability of similarities (distances) characteristics of relief segments grouped into 6 groups in the year 2010.

Group	n *	Area (ha)	Area (%)	Min	Max	Mean	Standard Deviation
1	85	7.70	18.55	0.003	0.657	0.125	0.086
2	16	1.14	2.75	0.017	0.459	0.192	0.099
3	40	1.48	3.57	0.008	0.374	0.125	0.070
4	62	29.49	71.04	0.003	0.541	0.122	0.077
5	6	1.55	3.73	0.006	0.183	0.093	0.066
6	4	0.15	0.36	0.004	0.142	0.073	0.061
Total	213	41.51	100.00	0.003	1.000	0.283	0.226

* Number of segments.

3.1.2. The Situation in 2013

Scott's 2013 valley floor model was divided into 175 segments, grouped into 5 groups. By far the most numerous (73 segments), and occupying the largest area, are those segments in Group 2 (36.29 ha; 87.42%) covering almost the entire valley floor, except for the outwash plain, throat (upper gorge) and fragments of alluvial fan (Figure 4A,B). In its internal structure (Figure 4A), 3 larger subgroups are visible. Despite this large area and variation in dendrogram structure, it stands out for having the lowest mean distance (Table 2) which indicates the greatest internal similarity. It also has one of the lower standard deviations. The second largest in terms of area is Group 1 (2.11 ha; 5.08%), which has a significant number of segments (57). It covers entire sections of the upper and lower gorges and appears sporadically in the marginal zone of the entire valley floor. Group 3 (12 segments) is the third in terms of area. Its occurrence is limited to the sedimentary basin, which speaks for the uniqueness of the relief of this area. But the high max-distance and standard deviation values indicate that it is strongly internally differentiated. Group 4 (18 segments) is flanked by Group 3 and forms a narrow zone in the outer part of the alluvial fan. The smallest area (0.24 ha; 0.58%) is occupied by Group 5 (15 segments). It does not form dense areas and occurs as individual tiles on the margins of the valley floor.

Table 2. Area and changeability of similarity (distance) characteristics of relief segments grouped into 5 groups in 2013.

Group	n *	Area (ha)	Area (%)	Min	Max	Mean	Standard Deviation
1	57	2.11	5.08	0.006	0.433	0.129	0.073
2	73	36.29	87.42	0.001	0.569	0.111	0.079
3	12	1.97	4.75	0.007	0.674	0.200	0.161
4	18	0.90	2.17	0.025	0.500	0.168	0.090
5	15	0.24	0.58	0.009	0.421	0.170	0.111
Total	175	41.51	100.00	0.002	0.288	0.998	0.236

* Number of segments.

3.2. Relief Similarity and Change Detection

The similarity map (Figure 5B), created by comparing the 2010 and 2013 geomorphic maps, illustrates the degree of similarity calculated for the surface motifs from these years, which can also be interpreted as the degree of relief change. Very clear on the map are zones where the relief has hardly changed (red colour; 0.95–1.00). These are compact areas located mainly below the gorge, on the inflow cone and in the form of a shelf in the upper, eastern part of the valley. It occupies the largest area (Table 3), accounting for 55.2% of the whole. Small but visible changes (orange colour; 0.90–0.95) occurred in 17.2% of the area and are located in the upper part of the valley and in the zone of troughs dissecting the lower part of the valley and a fragment of the alluvial fan. They do not form dense areas

and are generally intermixed with areas of slightly greater variation (yellow; 0.80–0.90), occupying 14.84% of the valley floor. A larger proportion of the surface (6.01%) still has cells with a degree of similarity in the range 0.70–0.80 (light yellow–light blue). They occur mainly in the upper part of the valley, intermixed with other categories. The remaining categories (0.00–0.70; shades of blue) cover a total of 6.01% of the area. They are most pronounced in the area of the flow-through lake, within outwash plain and in the lower section of the trough cutting the alluvial fan.

Figure 4. Dendrogram (**A**) and map (**B**) of relief segments (2013) grouped into 5 main groups. The dotted line on the dendrogram (**A**) marks the height of cutting.

In order to trace, in depth, the changes in relief depicted by the geomorphons, four examples (Figure 5A) representing areas of varying degrees of change (Figure 6) have been collated under magnification. Example 1 comprises the terrace on the eastern side of the upper valley section (Figure 6J–L). This is an area where no significant changes in relief have been recorded. Example 2 covers the active valley floor above the gorge, where changes are legible, but there are also motifs with no change (Figure 6G–I). Example 3 (Figure 6D–F) is the zone of the flow-through lake that develops annually in the inlet to the upper gorge during the melt season and acts as a sediment trap for sediments routed from the glacier and from the outwash plain, where changes are greatest and where there are motifs with low similarity in the range 0.0–0.15. Example 4 is the zone of the active channel

in the lower valley section (Figure 6A–C). This is a surface where areas of weak but legible change occur alongside motifs with no change.
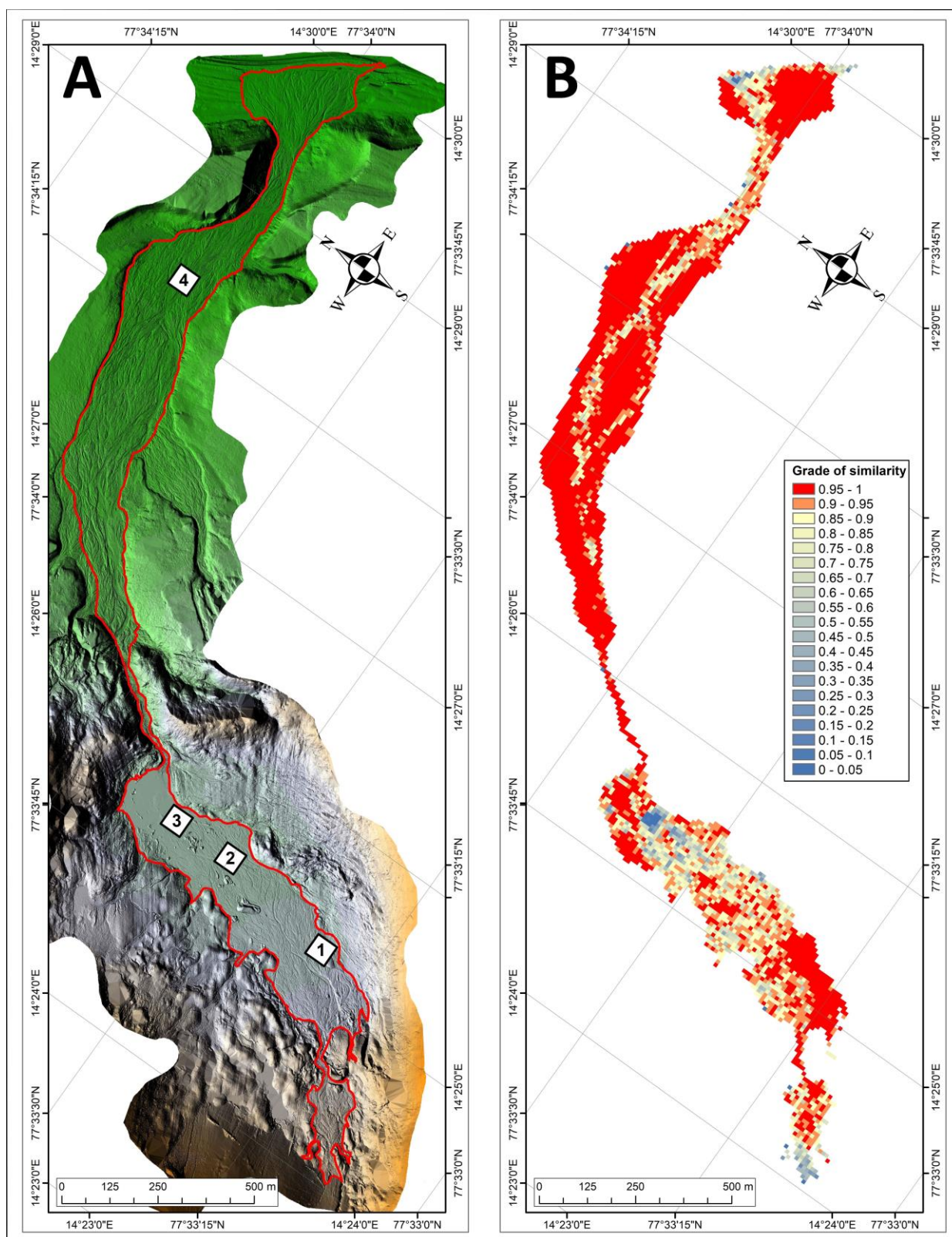

Figure 5. Digital terrain model (**A**) and map of similarity (**B**). Small frames with numbers show the extent of the sampled geomorphon and similarity maps presented in Figure 6.
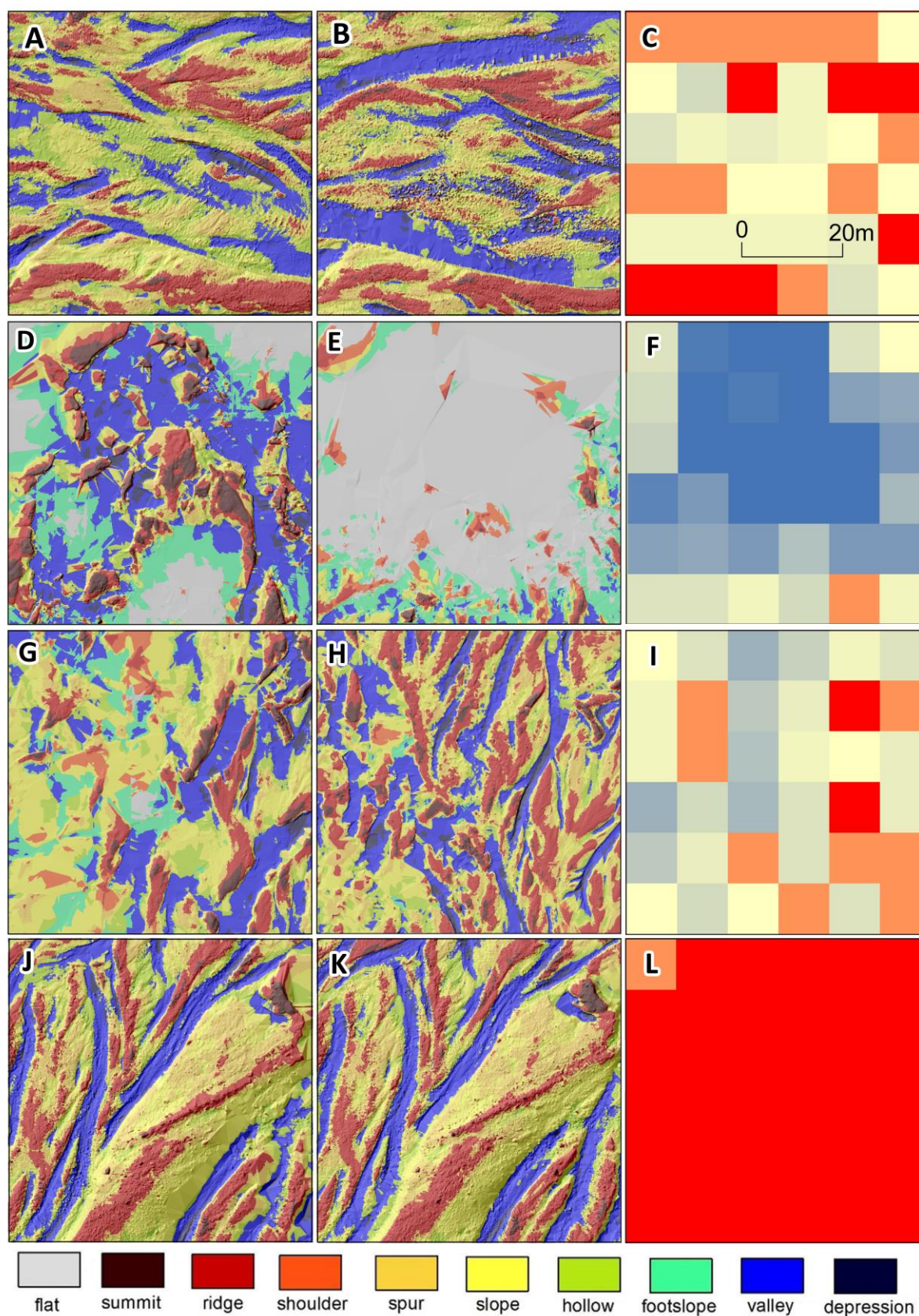
Figure 6. Maps of geomorphons in 2010 (**A,D,G,J**) and 2013 (**B,E,H,K**) and their similarity (**C,F,I,L**). Figures (**A–C**) present the area of frame 4, (**D–F**) present the area of frame 3, (**G–I**) present the area of frame 2, and (**J–L**) present the area of frame 1. Extent of frames and scale of similarity are presented in Figure 5A.

Table 3. Area of similarities (distances) in ranges of values.

Range Number	Range	*n* *	% (Area)	Area (ha)
1	0.00–0.05	7	0.17	0.07
2	0.05–0.10	3	0.07	0.03
3	0.10–0.15	3	0.07	0.03
4	0.15–0.20	4	0.10	0.04
5	0.20–0.25	3	0.07	0.03
6	0.25–0.30	15	0.36	0.15
7	0.30–0.35	14	0.34	0.14
8	0.35–0.40	6	0.14	0.06
9	0.40–0.45	15	0.36	0.15
10	0.45–0.50	22	0.53	0.22
11	0.50–0.55	28	0.68	0.28
12	0.55–0.60	44	1.06	0.44
13	0.60–0.65	36	0.87	0.36
14	0.65–0.70	80	1.93	0.80
15	0.70–0.75	113	2.73	1.13
16	0.75–0.80	136	3.28	1.36
17	0.80–0.85	215	5.19	2.15
18	0.85–0.90	400	9.65	4.00
19	0.90–0.95	713	17.20	7.13
20	0.95–1.00	2,289	55.20	22.89
	Total	4,162	100.00	41.62

* number of cells.

4. Discussion

To date, studies of relief changes in areas characterised by highly dynamic geomorphic processes have been conducted using mainly traditional field methods (geological and geomorphological mapping), have been typically limited to smaller areas and have had a qualitative character [39,40]. A much larger area of geomorphological mapping of subglacial areas has been achieved through the use of satellite imagery [41,42] and aerial photographs [43,44]. However, due to their small scale, their results are of rather an overview character. Very few studies have combined photo-interpretation methods with field surveys [45]. Technological advances and the increased availability of high-resolution elevation data [19–21], have resulted in a change in approach to the assessment of changes in relief [15,46]. A more recent trend is the use of high-resolution DTMs, developed from traditional (airborne) and UAV-derived low-altitude aerial imagery, for mapping, with verification undertaken on the basis of terrain mapping performed with GNSS receivers [46,47]. UAVs are now increasingly being used for detailed terrain mapping [47]. LiDAR-derived surveying technologies (TLS, ALS) now provide high-quality elevation data that can be acquired for larger areas [22]. An example is the National Guard Information System (ISOK) programme covering Poland, which provides LiDAR data with a density of 4 to 12 pts/km^2 [48], allowing the creation of DTMs with a resolution of 1 m [49]. The implementation of specialised GIS tools for the analysis of these elevation models enables quantitative estimation of changes in the topography, and the use of geomorphometric methods extends and details these studies [30]. TLS-derived high resolution DTMs and their derivatives are changing the way geomorphologists study relief and its evolution, contributing to a more efficient conceptualization of landforms by studying their pattern, spatial variation and relief changes. The classification of terrain morphology using geomorphons, proposed by Jasiewicz and Stepinski [25,26], enables the rapid and accurate description of morphology patterns over large areas. This type of topographic texture analysis facilitates the understanding of the relationships between the distribution of geomorphometric features, activity of geomorphic processes and relief changes and similarities [30].

There are few studies focused on studying the relief changes of glacier valley bottoms using geomorphometric methods. A quantitative evaluation of relief was carried out using

geomorphometric objects, identified using high resolution DTMs and the geomorphons method, GeoPAT2 software and algorithms of segmentation, and hierarchical clustering and similarity measures [36].

The proposed framework allows for a detailed analysis of relief based on the similarity of designated motifs and relief segments, the end result of which is a relief classification, distinguishing areas of similar relief and their changes. This paper presents analyses at a local scale (0.42 km^2 area) based on high-resolution (0.1 m) DTM. The use of such high accuracy data has made it possible to classify landforms (topography) in places in which they are usually of small (vertical and horizontal) size, making their inventory impossible to perform with traditional (field) methods over a larger area. The two geomorphon maps obtained, representing the topography pattern in the 2010 and 2013 survey seasons, provided the basis for a quantitative analysis of the similarity and changes in relief that occurred in this dynamic environment over a three-year period.

Analyses performed over a three-year timespan (2010–2013) have revealed that there are several zones in the Scott River valley floor characterized by varying degrees of relief reshaping. The area located in the upper section of the valley (above the upper gorge) has undergone the greatest changes. This is a glacier foreland zone limited by a terminal moraine rampart, from which the Scottbreen has successively retreated over the past century [50]. There are no clear zones characterized by low or high similarity. The mosaic of landforms makes everything seem "mixed." (Figure 5). Only one of the relatively homogeneous areas characterised by low change, covering the S part of the foreland, stands out. This spatial pattern is arguably the result of the periodic barricading of the upper gorge by ice at the beginning of the melt season. The ice blocking the outflow usually melts out by the end of June, providing the boost for intense bottom reshaping. Consequently, channels in this zone function periodically, and many are re-formed yearly after the outflow is unblocked. When valley glaciers terminate on land, the typical situation is that flow-through lakes function on their foreland, performing the function of sediment traps [11,51]. This is also the case in the upper section of the Scott River valley floor, with periodic development of a flow-through lake. In addition to trapping sediment transported by proglacial waters, it also performs the function of a discharge regulator that buffers the flow of meltwater and sediment from the glacier, foreland and outwash plain into the middle and lower valley sections [13]. A different mechanism shapes the zone in the close vicinity of the Scott Glacier terminus, where a strip of forefield tens of meters wide is exposed from under the ice every year. Here, unconsolidated sediments from the glacier's surface and sub-surface form ephemeral landforms that undergo dynamic reshaping during the melt season [7]. In contrast, the very narrow rock throat of the upper gorge shows a very high grade of similarity. In this throat, which narrows to less than 10 m in some places, proglacial waters do not have the opportunity to form a complex channel pattern. Probably for this reason, therefore, the relief here is stable. Below the upper gorge, the situation progressively changes. In the narrow higher section, there is almost no change in relief. Although channel patterns are evident in the relief of the bottom, they are not included in the zone of active outflow during the melt season. Located higher than the seasonal channel pattern, these are only activated during the highest floods [52]. As the valley floor widens, the pattern of the channels changes, indicating an increase in geomorphic processes. The changes in the channel pattern, recorded in the middle section, are the result of the intensification of erosion and deposition processes (lateral erosion, downcutting, bank and bed erosion, sediment mobilization and deposition) observed in small polar catchments. The intensity and course of these processes are closely linked to the availability and supply of sediment [13,52–55]. The currently observed transformations in the Scott River catchment, manifested by the predominance of erosion over aggradation, are a characteristic feature of preglacial rivers [55,56]. The low grade of similarity in this section indicates significant changes in the trough pattern (shift and avulsion) of flow during successive melt seasons. In this zone, the Scott River splits into two channels distinguished by a lower grade of similarity. However, these changes apply only to the

zone of seasonal channel activity. The higher-lying, marginal parts of the bed remain stable. Further downstream, in the lower gorge, the situation changes again and almost the entire section of the lower gorge has 'mixed' segments with varying degrees of similarity. This is the result of the narrowing of the valley floor from 250–300 m in the middle section, to 50 m in the lower gorge. The Scott River is forced to reconfigure channel patterns that join to a single channel functioning for a majority of the melt season. At the same time, during flood events, waters cover most of the valley floor, leading to intense channel and bars reshaping [57,58]. Additionally, downstream (below the lower gorge) of the northern part of the alluvial fan stands out, as the grade of similarity is very low in some places. A small lagoon forms here every year, which receives water from both the main channel and the distribution channels [59]. The rest of the alluvial fan area is stable.

5. Conclusions

The relief changes study was carried out in an area of unglaciated Scott Valley floor (0.42 km^2), 3.3 km long, located in the NW part of Wedel Jarlsberg Land (SW Spitsbergen). It is an area strongly reshaped by proglacial waters flowing from beneath the glacier terminus occupying the SW part of the valley.

The study used high-resolution (0.1 m) DTMs developed from TLS survey data acquired during the 2010 and 2013 summer seasons. The DTMs were processed into geomorphon maps, which were used to analyse the relief similarity in each year and the relief changes that occurred between measurements.

In the first step, relief segments maps were generated using GeoPAT2 software and the R system, delineating areas of high similarity, for each year separately. In a second step, the geomorphon maps were used to analyse the similarity of relief between seasons. Grade of similarity was interpreted as relief changes, i.e., where similarity was high, relief changes were considered to have been small, whereas surfaces with a low degree of similarity appear to have been actively modelled by geomorphic processes.

In each of the seasons analysed, the picture of relief was similar, but significant differences were also marked. In the 2010 season, 213 segments of relief were grouped into 6 classes. In 2013, the segments were fewer (175) and there were five groups. The year 2010 is distinguished from 2013 in relief by the strong fragmentation of the upper section of the valley floor, where the presence of segments from four groups is clearly marked. In each season, the presence of separate groups of segments covering the upper gorge and flow-through lake in the upper valley section is characteristic.

The analysis of similarity of relief for both study seasons allowed us to distinguish the zones characterised by relief stability, which occupy more than 50% of the area and are the outer zones of the valley bottom. Weakly active zones occupy the upper part of the bottom (above the gorge) and the flow-through zone along the whole valley section. The most active and transformed part is the immediate foreland of the Scott Glacier front, the flow-through lake zone and the lower part of the alluvial fan.

The proposed method provides new opportunities for the accurate monitoring of qualitative changes in terrain morphology, which is especially useful in areas that are difficult to directly access, such as proglacial braided valley bottoms and channels. High-resolution elevation data acquired during two measurement seasons by remote sensing methods (TLS), have allowed us to capture and estimate changes in morphology that are difficult to record by traditional field methods, and to describe these changes using geomorphometric methodology. The analyses also allow us to separate groups of surfaces characterized by morphological similarity, as a consequence of the comparable geomorphological processes that led to their shaping. The advantage of this method is the ability to cover much larger areas with analyses than in the case of traditional field mapping. This can be used in all areas for which high-resolution digital terrain models are available.

References

1. *Snow, Water, Ice and Permafrost in the Arctic (SWIPA): Climate Change and the Cryosphere*; AMAP: Oslo, Norway, 2011; ISBN 978-82-7971-071-4.
2. Amélineau, F.; Grémillet, D.; Harding, A.M.A.; Walkusz, W.; Choquet, R.; Fort, J. Arctic Climate Change and Pollution Impact Little Auk Foraging and Fitness across a Decade. *Sci. Rep.* **2019**, *9*, 1014. [CrossRef]
3. Vaughan, D.G.; Comiso, J.C.; Allison, I.; Carrasco, J.; Kaser, G.; Kwok, R.; Mote, P.; Murray, T.; Paul, F.; Ren, J.; et al. Observations: Cryosphere. *Clim. Chang.* **2013**, *2103*, 317–382.
4. Kääb, A.; Berthier, E.; Nuth, C.; Gardelle, J.; Arnaud, Y. Contrasting Patterns of Early Twenty-First-Century Glacier Mass Change in the Himalayas. *Nature* **2012**, *488*, 495–498. [CrossRef]
5. Woul, M.D.; Hock, R. Static Mass-Balance Sensitivity of Arctic Glaciers and Ice Caps Using a Degree-Day Approach. *Ann. Glaciol.* **2005**, *42*, 217–224. [CrossRef]
6. Arheimer, B.; Lindström, G. Climate Impact on Floods: Changes in High Flows in Sweden in the Past and the Future (1911–2100). *Hydrol. Earth Syst. Sci.* **2015**, *19*, 771–784. [CrossRef]
7. Kociuba, W.; Gajek, G.; Franczak, Ł. A Short-Time Repeat TLS Survey to Estimate Rates of Glacier Retreat and Patterns of Forefield Development (Case Study: Scottbreen, SW Svalbard). *Resources* **2020**, *10*, 2. [CrossRef]
8. Ashworth, P.J.; Ferguson, R.I. Interrelationships of Channel Processes, Changes and Sediments in a Proglacial Braided River. *Geogr. Ann. Ser. A Phys. Geogr.* **1986**, *68*, 361–371. [CrossRef]
9. Ashworth, P.J.; Best, J.L.; Jones, M. Relationship between Sediment Supply and Avulsion Frequency in Braided Rivers. *Geology* **2004**, *32*, 21. [CrossRef]
10. Carrivick, J.L.; Geilhausen, M.; Warburton, J.; Dickson, N.E.; Carver, S.J.; Evans, A.J.; Brown, L.E. Contemporary Geomorphological Activity throughout the Proglacial Area of an Alpine Catchment. *Geomorphology* **2013**, *188*, 83–95. [CrossRef]
11. Beylich, A.A.; Laute, K. Sediment Sources, Spatiotemporal Variability and Rates of Fluvial Bedload Transport in Glacier-Connected Steep Mountain Valleys in Western Norway (Erdalen and Bødalen Drainage Basins). *Geomorphology* **2015**, *228*, 552–567. [CrossRef]
12. Ashworth, P.J.; Best, J.L.; Jones, M.A. The Relationship between Channel Avulsion, Flow Occupancy and Aggradation in Braided Rivers: Insights from an Experimental Model. *Sedimentology* **2007**, *54*, 497–513. [CrossRef]
13. Kociuba, W. Assessment of Sediment Sources throughout the Proglacial Area of a Small Arctic Catchment Based on High-Resolution Digital Elevation Models. *Geomorphology* **2017**, *287*, 73–89. [CrossRef]
14. Kociuba, W.; Krzążek, P.; Superson, J. Combining GPS-RTK and rephotographic methodolo-gies for the assessment of transformations of the ephemeral landforms of the near foreland of a valley glacier (Scottbreen, Svalbard). *Z. Geomorphol.* **2016**, *60*, 29–44. [CrossRef]
15. Chandler, B.M.P.; Lovell, H.; Boston, C.M.; Lukas, S.; Barr, I.D.; Benediktsson, Í.Ö.; Benn, D.I.; Clark, C.D.; Darvill, C.M.; Evans, D.J.A.; et al. Glacial Geomorphological Mapping: A Review of Approaches and Frameworks for Best Practice. *Earth-Sci. Rev.* **2018**, *185*, 806–846. [CrossRef]
16. Kääb, A.; Lefauconnier, B.; Melvold, K. Flow field of Kronebreen, Svalbard, using repeated Landsat 7 and ASTER data. *Ann. Glaciol.* **2005**, *42*, 7–13. [CrossRef]
17. Brasington, J.; Rumsby, B.T.; McVey, R.A. Monitoring and Modelling Morphological Change in a Braided Gravel-Bed River Using High Resolution GPS-Based Survey. *Earth Surf. Process. Landf.* **2000**, *25*, 973–990. [CrossRef]

18. Charlton, M.E.; Large, A.R.G.; Fuller, I.C. Application of Airborne LiDAR in River Environments: The River Coquet, Northumberland, UK. *Earth Surf. Process. Landf.* **2003**, *28*, 299–306. [CrossRef]

19. Bamber, J.L.; Krabill, W.; Raper, V.; Dowdeswell, J.A.; Oerlemans, J. Elevation Changes Measured on Svalbard Glaciers and Ice Caps from Airborne Laser Data. *Ann. Glaciol.* **2005**, *42*, 202–208. [CrossRef]

20. Arnold, N.S.; Rees, W.G.; Devereux, B.J.; Amable, G.S. Evaluating the Potential of High-resolution Airborne LiDAR Data in Glaciology. *Int. J. Remote Sens.* **2006**, *27*, 1233–1251. [CrossRef]

21. Glenn, N.F.; Streutker, D.R.; Chadwick, D.J.; Thackray, G.D.; Dorsch, S.J. Analysis of LiDAR-Derived Topographic Information for Characterizing and Differentiating Landslide Morphology and Activity. *Geomorphology* **2006**, *73*, 131–148. [CrossRef]

22. Heritage, G.L.; Milan, D.J.; Large, A.R.G.; Fuller, I.C. Influence of Survey Strategy and Interpolation Model on DEM Quality. *Geomorphology* **2009**, *112*, 334–344. [CrossRef]

23. Kociuba, W.; Kubisz, W.; Zagórski, P. Use of Terrestrial Laser Scanning (TLS) for Monitoring and Modelling of Geomorphic Processes and Phenomena at a Small and Medium Spatial Scale in Polar Environment (Scott River—Spitsbergen). *Geomorphology* **2014**, *212*, 84–96. [CrossRef]

24. Bangen, S.G.; Wheaton, J.M.; Bouwes, N.; Bouwes, B.; Jordan, C. A Methodological Intercomparison of Topographic Survey Techniques for Characterizing Wadeable Streams and Rivers. *Geomorphology* **2014**, *206*, 343–361. [CrossRef]

25. Stepinski, T.F.; Jasiewicz, J. Geomorphons—A New Approach to Classification of Landforms. *Proc. Geomorphometry*. 2011, pp. 109–112. Available online: https://geomorphometry.org/wp-content/uploads/2021/07/StepinskiJasiewicz2011geomorphometry.pdf (accessed on 16 October 2023).

26. Jasiewicz, J.; Stepinski, T.F. Geomorphons—A Pattern Recognition Approach to Classification and Mapping of Landforms. *Geomorphology* **2013**, *182*, 147–156. [CrossRef]

27. Dąbrowski, A.; Jasiewicz, J. Zastosowanie Form Morfometrycznych Do Analizy Zróżnicowania Wybranych Typów Powierzchni na Obszarach Młodoglacjalnych. Badania fizjograficzne **2014**, R. V seria A, 095-111, Poznańskie Towarzystwo Przyjaciół Nauk oraz Wydziału Nauk Geograficznych i Geologicznych i Wydziału Biologii Uniwersytetu im. Adama Mickiewicza w Poznaniu, Poznań, Poland. Available online: https://repozytorium.amu.edu.pl/server/api/core/bitstreams/1c6c790e-5d86-4f5f-865b-f91c04f9c35d/content (accessed on 19 October 2023).

28. Jasiewicz, J.; Netzel, P.; Stepinski, T.F. Landscape Similarity, Retrieval, and Machine Mapping of Physiographic Units. *Geomorphology* **2014**, *221*, 104–112. [CrossRef]

29. Gawrysiak, L. *Segmentacje Rzeźby Terenu z Wykorzystaniem Metod Automatycznej Klasyfikacji i ich Relacja do Mapy Geomorfologicznej*; MCSU Press: Lublin, Poland, 2018.

30. Gawrysiak, L.; Kociuba, W. Application of Geomorphons for Analysing Changes in the Morphology of a Proglacial Valley (Case Study: The Scott River, SW Svalbard). *Geomorphology* **2020**, *371*, 107449. [CrossRef]

31. Bartoszewski, S.; Gluza, A.; Siwek, K.; Zagórski, P. Temperature and Rainfall Control of Outflow from the Scott Glacier Catchment (Svalbard) in the Summers of 2005 and 2006. *Nor. Geogr. Tidsskr.-Nor. J. Geogr.* **2009**, *63*, 107–114. [CrossRef]

32. Harasimiuk, M.; Gajek, G. Tectonic and lithology. In *Geographical Environment of NW Part of Wedel Jarlsberg Land (Spitsbergen, Svalbard)*; Zagórski, P., Harasimiuk, M., Rodzik, J., Eds.; MCSU Press: Lublin, Poland, 2013; pp. 34–47.

33. Leica-Geosystems. Leica ScanStation C10—Datasheet. 2012. Available online: https://www.geooptic.ru/static/files/leica-scanstation-c10-ds.pdf (accessed on 30 August 2023).

34. Smith, M.W.; Vericat, D. Evaluating Shallow-Water Bathymetry from Through-Water Terrestrial Laser Scanning Under a Range of Hydraulic and Physical Water Quality Conditions. *River Res. Apps* **2014**, *30*, 905–924. [CrossRef]

35. Zhang, W.; Qi, J.; Wan, P.; Wang, H.; Xie, D.; Wang, X.; Yan, G. An Easy-to-Use Airborne LiDAR Data Filtering Method Based on Cloth Simulation. *Remote Sens.* **2016**, *8*, 501. [CrossRef]

36. Netzel, P.; Nowosad, J.; Jasiewicz, J.; Niesterowicz, J.; Stepinski, T. Geopat 2: User's Manual. *2018, 521.* Available online: https://zenodo.org/records/1291123/files/GeoPAT2_Manual.pdf?download=1 (accessed on 19 October 2023).

37. Haralick, R.M.; Shanmugam, K.; Dinstein, I. Textural Features for Image Classification. *IEEE Trans. Syst. Man. Cybern.* **1973**, *SMC-3*, 610–621. [CrossRef]

38. Lin, J. Divergence Measures Based on the Shannon Entropy. *IEEE Trans. Inform. Theory* **1991**, *37*, 145–151. [CrossRef]

39. Gogołek, W.; Lewandowski, W. Preliminary geomorphological characteristic of Linnedalen (Spitsbergen, Svalbard Archipelago). *Pol. Polar Res.* **1980**, *1*, 7–19.

40. Lacika, J.; Musiał, A. Relief-forming processes in the polar zone. Example from Nordenskiold Land (West Spitsbergen). *Misc. Geogr* **1988**, *3*, 69–78. [CrossRef]

41. Ewertowski, M.W.; Evans, D.J.A.; Robertsaand, D.H.; Tomczyk, A.M. Glacial geomorphology of the terrestrial margins of the tidewater glacier, Nordenskiöldbreen, Svalbard. *J. Maps* **2016**, *12*, 476–487. [CrossRef]

42. Tomczyk, A.; Ewertowski, M.W. Surface morphological types and spatial distribution of fan-shaped landforms in the periglacial high-Arctic environment of central Spitsbergen, Svalbard. *J. Maps* **2017**, *13*, 239–251. [CrossRef]

43. Jania, J.; Szczypek, T. Geomorphological mapping of the Hornsund fjord region from interpretation of aerial photographs. *Fotointerpret. W Geogr.* **1987**, *19*, 9108–9128.

44. Szczęsny, R. Quaternary landforms and deposits in southern Spitsbergen on the ground of photointerpretation. *Pol. Polar Res.* **1991**, *12*, 289–343.

45. Karczewski, A.; Andrzejewski, L.; Chmal, H.; Jania, J.; Kłysz, P.; Kostrzewski, A.; Lindner, L.; Marks, L.; Pękala, K.; Pulina, M.; et al. *Hornsund, Spitsbergen. Geomorphology. 1:75 000 (Map)*; Silesian University: Katowice, Poland, 1984.

46. Allaart, L.; Schomacker, A.; Håkansson, L.M.; Farnsworth, W.R.; Brynjólfsson, S.; Grumstad, A.; Kjellman, S.E. Geomorphology and surficial geology of the Femmilsjøen area, northern Spitsbergen. *Geomorphology* **2021**, *382*, 107693. [CrossRef]

47. Ewertowski, M.W.; Tomczyk, A.M.; Evans, D.J.A.; Roberts, D.H.; Ewertowski, W. Operational Framework for Rapid, Very-High Resolution Mapping of Glacial Geomorphology Using Low-Cost Unmanned Aerial Vehicles and Structure-from-Motion Approach. *Remote Sens.* **2019**, *11*, 65. [CrossRef]

48. Woźniak, P. High Resolution Elevation Data in Poland. In *Geomorphometry for Geosciences*; Adam Mickiewicz Uniwersity: Poznań, Poland, 2015; pp. 13–14.

49. Gawrysiak, L.; Kociuba, W. LiDAR-Derived Relief Typology of Loess Patches (East Poland). *Remote Sens.* **2023**, *15*, 1875. [CrossRef]

50. Rodzik, J.; Gajek, G.; Reder, J.; Zagórski, P. Glacial geomorphology. In *Geographical Environment of NW Part of Wedel Jarlsberg Land (Spitsbergen, Svalbard)*; Zagórski, P., Harasimiuk, M., Rodzik, J., Eds.; MCSU Press: Lublin, Poland, 2013; pp. 36–165.

51. Carrivick, J.L.; Berry, K.; Geilhausen, M.; James, W.H.M.; Williams, C.; Brown, L.E.; Rippin, D.M.; Carver, S.J. Decadal-scale Changes of the Ödenwinkelkees, Central Austria, Suggest Increasing Control of Topography and Evolution towards Steady State. *Geogr. Ann. Ser. A Phys. Geogr.* **2015**, *97*, 543–562. [CrossRef]

52. Kociuba, W.; Janicki, G.; Dyer, J.L. Contemporary Changes of the Channel Pattern and Braided Gravel-Bed Floodplain under Rapid Small Valley Glacier Recession (Scott River Catchment, Spitsbergen). *Geomorphology* **2019**, *328*, 79–92. [CrossRef]

53. Marren, P.M. Magnitude and Frequency in Proglacial Rivers: A Geomorphological and Sedimentological Perspective. *Earth-Sci. Rev.* **2005**, *70*, 203–251. [CrossRef]

54. Marren, P.M.; Toomath, S.C. Channel Pattern of Proglacial Rivers: Topographic Forcing Due to Glacier Retreat. *Earth Surf. Process. Landf.* **2014**, *39*, 943–951. [CrossRef]

55. Owczarek, P.; Nawrot, A.; Migała, K.; Malik, I.; Korabiewski, B. Flood-plain Responses to Contemporary Climate Change in Small H Igh-A Rctic Basins (S Valbard, N Orway). *Boreas* **2014**, *43*, 384–402. [CrossRef]

56. Cossart, É. Landform Connectivity and Waves of Negative Feedbacksduring the Paraglacial Period, a Case Study: The Tabuc Subcatchment since the End of the Little Ice Age (Massif Des Écrins, France). *Geomorphologie* **2008**, *14*, 249–260. [CrossRef]

57. Kociuba, W.; Janicki, G. Changeability of Movable Bed-surface Particles in Natural, Gravel-bed Channels and Its Relation to Bedload Grain Size Distribution (Scott River, Svalbard). *Geogr. Ann. Ser. A Phys. Geogr.* **2015**, *97*, 507–521. [CrossRef]

58. Kociuba, W. Geomorphic Changes of the Scott River Alluvial Fan in Relation to a Four-Day Flood Event. *Water* **2023**, *15*, 1368. [CrossRef]

59. Lehmann-Konera, S.; Kociuba, W.; Chmiel, S.; Franczak, Ł.; Polkowska, Ż. Effects of Biotransport and Hydro-Meteorological Conditions on Transport of Trace Elements in the Scott River (Bellsund, Spitsbergen). *PeerJ* **2021**, *9*, e11477. [CrossRef]